Supporting Information:

Exhaustive State-to-State Cross Sections for Reactive Molecular Collisions from Importance Sampling Simulation and a Neural Network Representation

Debasish Koner,[1] Oliver T. Unke,[1] Kyle Boe,[2] Raymond J. Bemish,[3] and Markus Meuwly[1, a)]

[1)] *Department of Chemistry, University of Basel, Klingelbergstrasse 80, CH-4056 Basel, Switzerland*

[2)] *Boston College, Institute for Scientific Research, Chestnut Hill, Massachusetts 02467, USA*

[3)] *Air Force Research Laboratory, Space Vehicles Directorate, Kirtland AFB, New Mexico 87117, USA*

(Dated: 7 May 2019)

[a)] m.meuwly@unibas.ch

I. QCT AND NN RATES

The QCT rates as a function of temperature are computed as

$$k(T) = g(T)\sqrt{\frac{8k_{\rm B}T}{\pi\mu}}\pi b_{\rm max}^2\frac{N_{\rm r}}{N_{\rm tot}}. \quad (1)$$

where $b_{\rm max}$ is the maximum impact parameter, $g(T)$ is the electronic degeneracy factor, $k_{\rm B}$ is the Boltzmann constant, μ is the reduced mass of the collision system $N_{\rm r}$ is the number of reactive trajectories of interest and $N_{\rm tot}$ is the total number of trajectories.

For the N(^{4}S)+NO(X$^2\Pi$) collision the degeneracy factor is[1]

$$g(T) = \frac{3}{4[2+2{\rm exp}(-177.1/T)]}. \quad (2)$$

The electronic partition function for N(^{4}4) is 4 and that for the NO molecule for two spin orbit states, 1/2 and 3/2 is $[2+2{\rm exp}(-177.1/T)]$. The term in the numerator is the electronic partition function for the ^{3}A$'$ state of N_2O.

The initial relative translational energies ($E_{\rm t}$) of the reactants are sampled from a Maxwell-Boltzmann distribution and the ro-vibrational states of NO at a particular temperature are sampled from Boltzmann distribution. The sampling procedures are discussed in detail in Refs. 2, 3 and 4.

The rates from the NN have been calculated according to

$$k(T) = g(T)\sqrt{\frac{8k_{\rm B}T}{\pi\mu}}\ \sigma_{\rm sum}. \quad (3)$$

Here $\sigma_{\rm sum}$ is the cross section calculated directly from the NN models, integrated either over the translational energy ($E_{\rm t}$) phase space (for initial state selected rates) or the $(v,j)-$state and the $E_{\rm t}$ phase space (for total rates) using Monte Carlo integration.

II. ADDITIONAL FIGURES

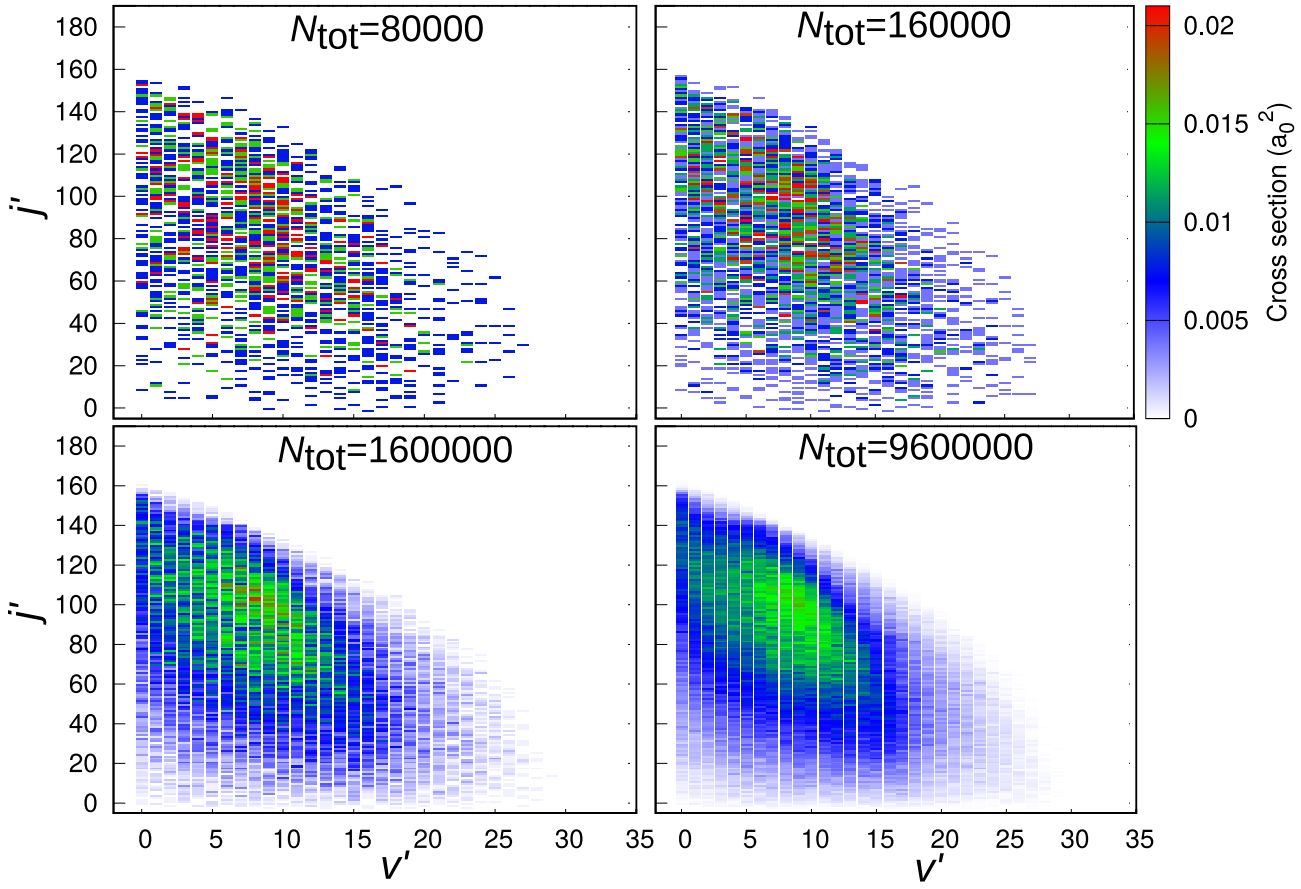

FIG. S1. State-to-state cross sections ($\sigma_{v,j\to v',j'}$) for N + NO($v = 6, j = 30$) → O + N_2(v', j') at $E_t = 2.5$ eV computed from different numbers of trajectories.

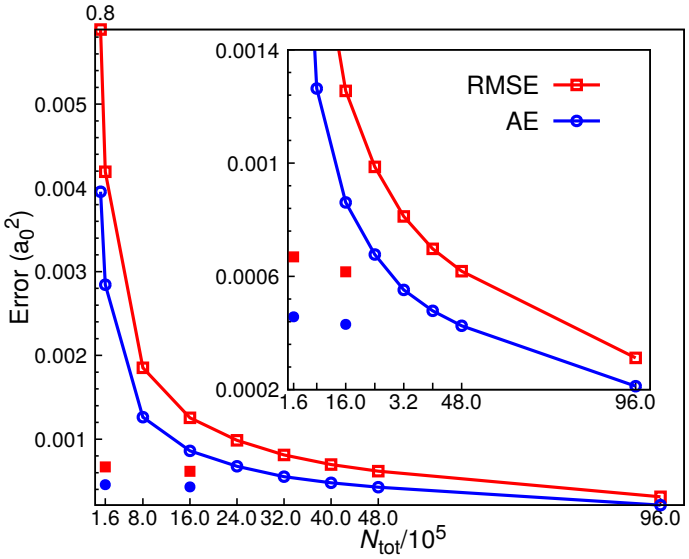

FIG. S2. Root mean square errors (RMSE, red) and absolute errors (AE, blue) for the state-to-state cross sections ($\sigma_{v,j\to v',j'}$) for N + NO($v = 6, j = 30$) $\to$ O + $N_2(v', j')$ at $E_t = 2.5$ eV computed from different numbers N_t of trajectories. Filled points at 1.6×10^6 show the errors obtained after local averaging and at 1.6×10^5 show the results obtained from biased sampling and local averaging. Unaveraged results obtained from 2×10^7 unbiased trajectories are used as reference data.

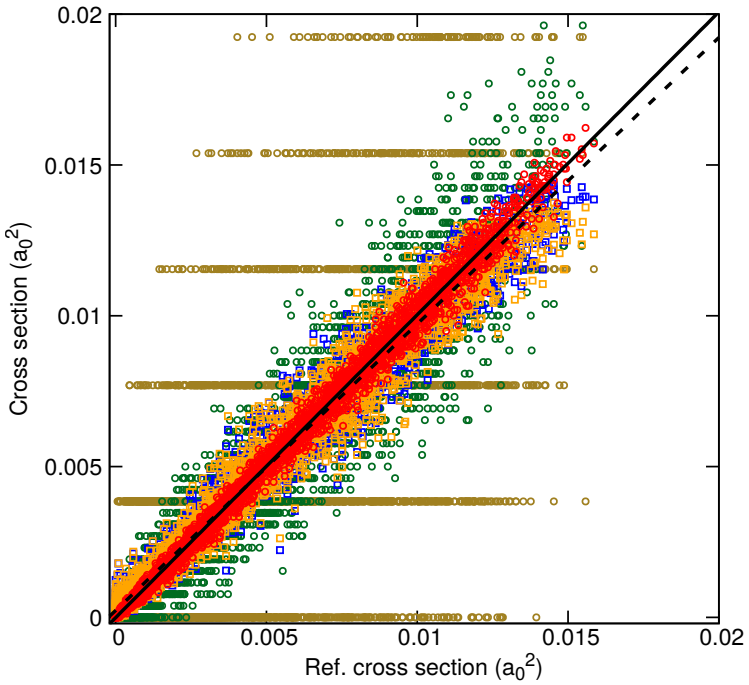

FIG. S3. Correlation between state-to-state cross sections ($\sigma_{v,j\to v',j'}$) for N + NO($v = 6, j = 30$) $\to$ O + $N_2(v', j')$ at $E_t = 2.5$ eV computed from different numbers of trajectories ($y-$axis) with the reference set ($N_{tot} = 2 \times 10^7$, $x-$axis). Circles represent the unaveraged results from unbiased simulations by running 1.6×10^5 (olive), 1.6×10^6 (dark green) and 9.6×10^6 (red) trajectories. Blue squares represent locally averaged results obtained from 1.6×10^6 trajectories while orange squares are locally averaged results obtained from 1.6×10^5 trajectories sampled using biased sampling. Linear least squares fit of red and orange data sets are shown as solid and dashed lines, respectively, and demonstrate the equivalence of the locally averaged results with the reference data. The olive circles (from $N_{tot} = 1.6 \times 10^5$ trajectories) are highly structured and far away from the reference data ($N_{tot} = 2 \times 10^7$) due to insufficient statistics (small number of reactive trajectories and hence low population of the product states).

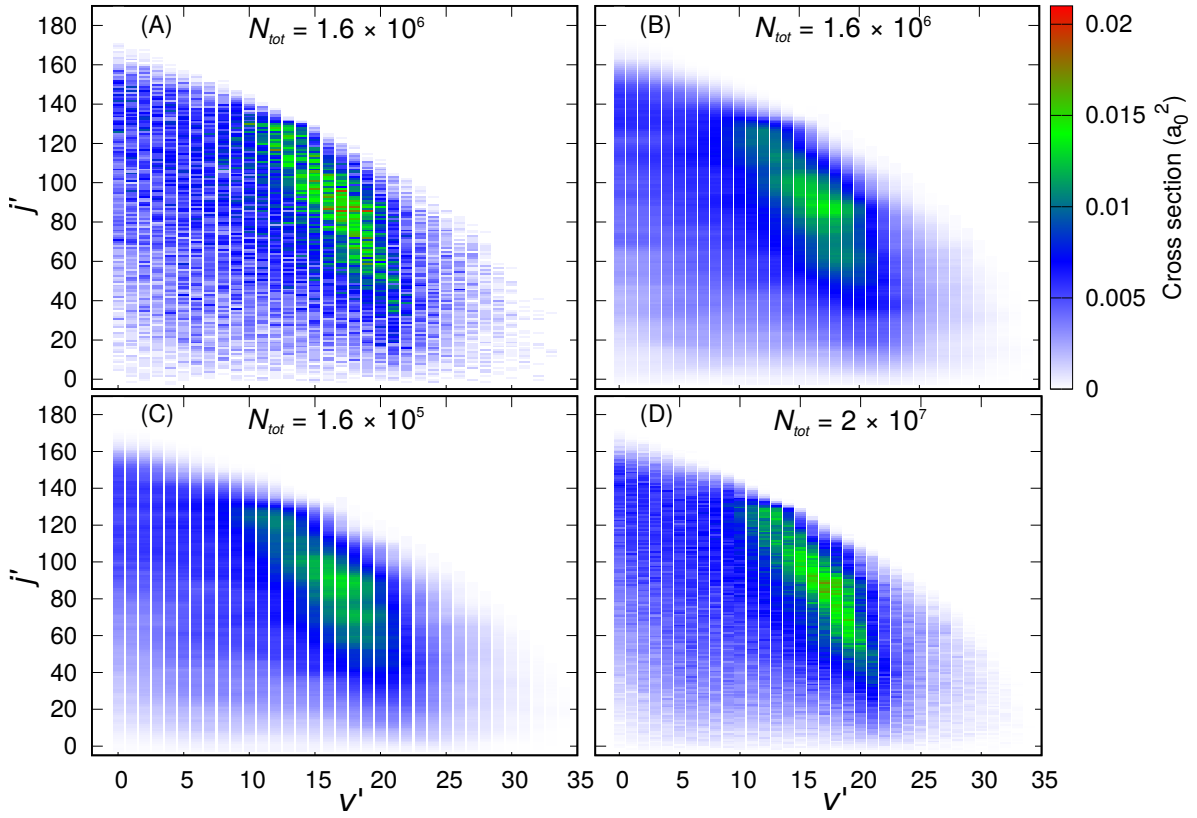

FIG. S4. State-to-state cross sections ($\sigma_{v,j\to v',j'}$) for N + NO($v = 10, j = 60$) → O + N_2(v', j') at E_t = 1.8 eV computed from different numbers of trajectories. Cross sections shown in panels (B) and (C) are averaged over neighbor states. In the panel (C) cross sections are obtained from trajectories sampled in b space via importance sampling.

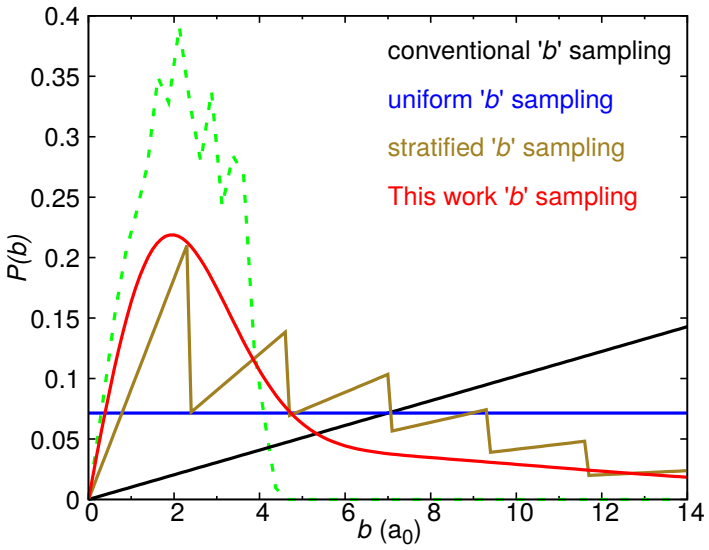

FIG. S5. Different impact parameter b-sampling schemes for QCT. The black, blue and olive lines show the distribution of impact parameter $P(b)$ sampled from conventional, uniform and stratified[2,3] sampling schemes. The red line shows $P(b)$ for the trajectories calculated to compute the state-to-state cross sections for $N + NO(v = 6, j = 30) \rightarrow O + N_2(v', j')$ at $E_t = 2.5$ eV. The green dashed line shows the contributions from the trajectories with different impact parameter to the total cross sections for these calculations.

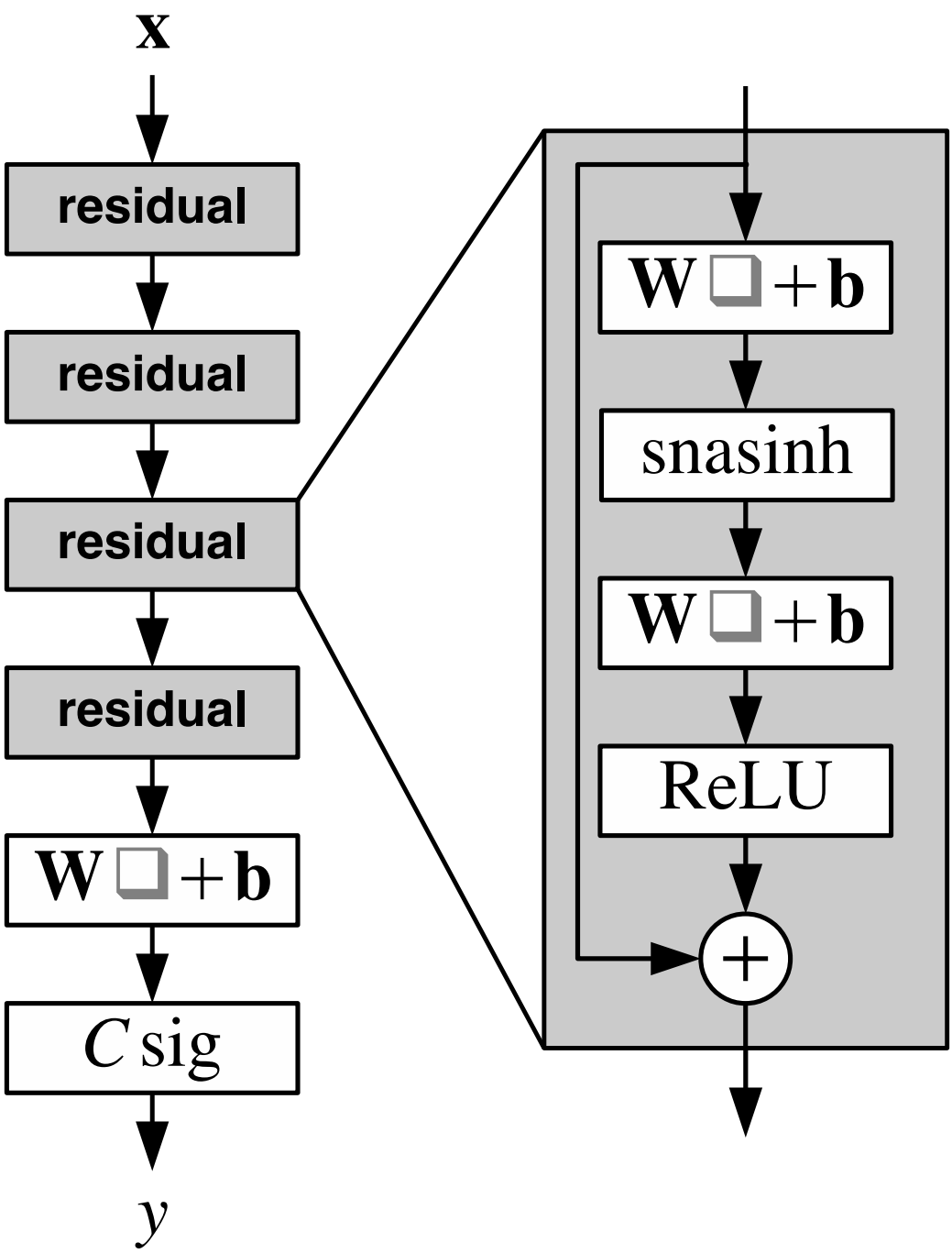

FIG. S6. Structure of the NN model used to train the cross sections.

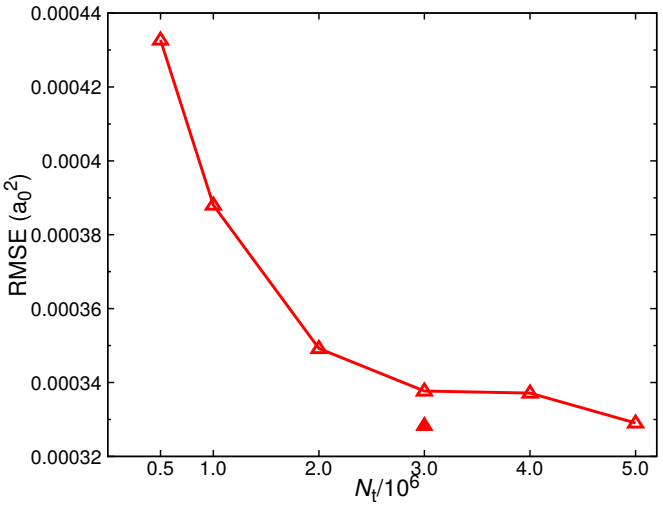

FIG. S7. Convergence of the NN-STS model with training set size N_t ("learning curve") for the NN-STS model measured from the root mean squared error for 2×10^5 test data set. Finally, $N_t = 3 \times 10^6$ was chosen for the final NN-STS model and trained extensively to obtain a low RMSE shown by the filled triangle.

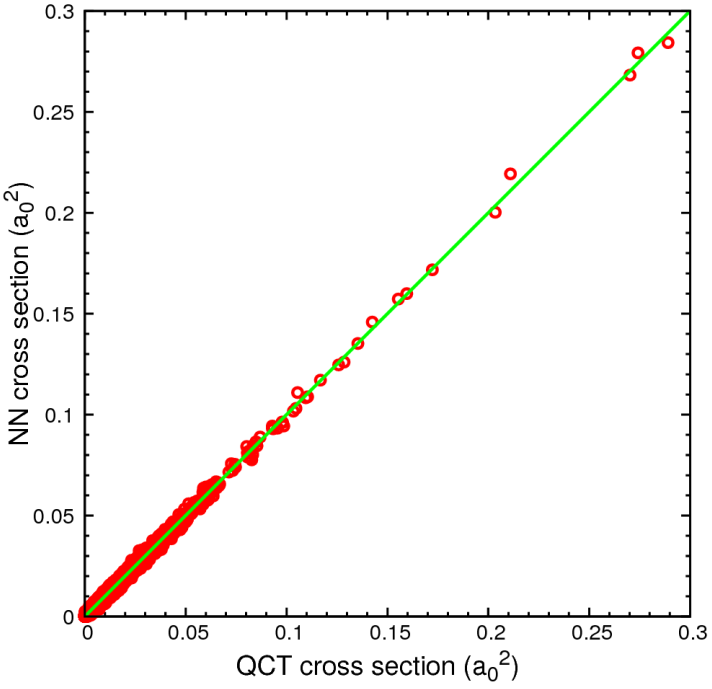

FIG. S8. Correlation between QCT-calculated (reference) and NN-STS predicted state-to-state cross sections for the test data. Diagonal is shown as green line.

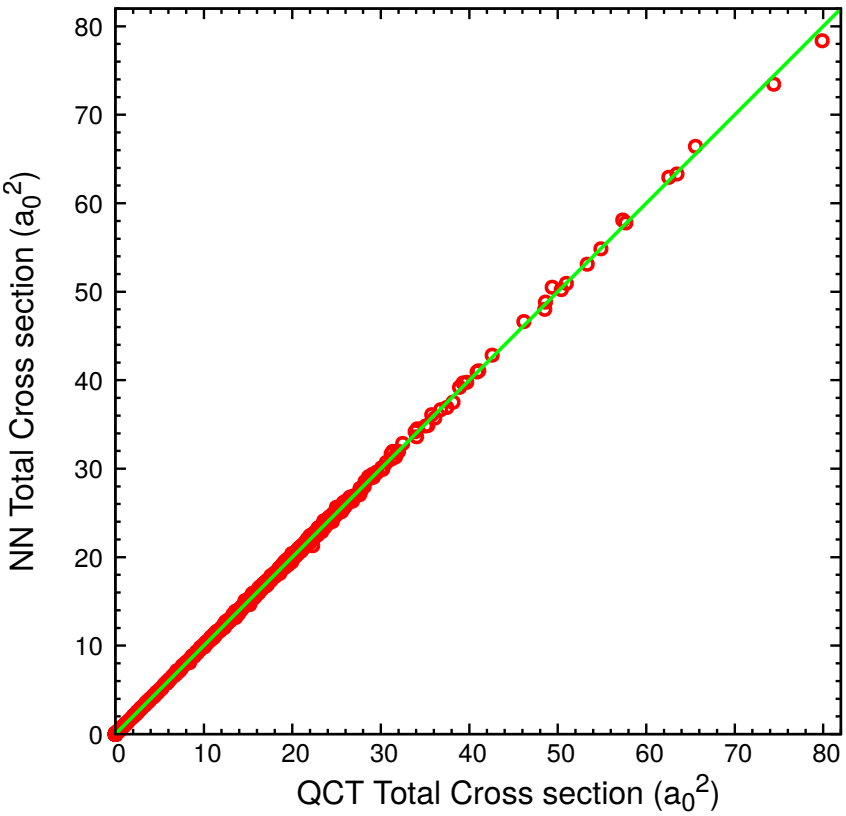

FIG. S9. Correlation between QCT-calculated (reference) and NN-Tot predicted total cross sections for the entire data set. Diagonal is shown as solid line.

TABLE S1. Initial state selected total reaction cross sections for N + NO$(v, j) \rightarrow$ O + N_2 at selected collision energies obtained via QCT calculations and from NN-STS and NN-Tot models.

v	j	E_t (eV)	σ_{QCT} (a_0^2)	$\sigma_{\mathrm{NN-STS}}$ (a_0^2)	$\sigma_{\mathrm{NN-Tot}}$ (a_0^2)
4	20	1.00	5.60	5.94	5.70
4	20	2.80	17.09	17.03	17.08
4	20	4.20	17.92	17.56	17.77
4	60	1.00	8.62	8.50	8.71
4	60	2.80	17.34	17.29	17.32
4	60	4.20	17.51	17.77	17.62
4	120	1.00	13.05	13.11	13.02
4	120	2.80	20.03	20.03	20.07
4	120	4.20	19.83	19.83	19.50
10	20	1.00	8.65	8.72	8.56
10	20	2.80	19.88	19.35	19.38
10	20	4.20	19.32	19.25	19.31
10	60	1.00	11.56	11.35	11.20
10	60	2.80	19.89	19.47	19.68
10	60	4.20	19.19	19.23	19.20
10	120	1.00	18.41	18.51	18.28
10	120	2.80	22.23	21.89	21.71
10	120	4.20	20.21	19.84	19.88
16	20	1.00	13.37	13.41	13.49
16	20	2.80	22.57	21.77	21.68
16	20	4.20	20.36	20.40	20.14
16	60	1.00	16.15	16.37	16.17
16	60	2.80	21.42	21.63	21.66
16	60	4.20	19.68	20.11	19.85
16	120	1.00	25.04	24.89	24.69
16	120	2.80	22.39	22.09	22.31
16	120	4.20	19.37	18.79	18.87

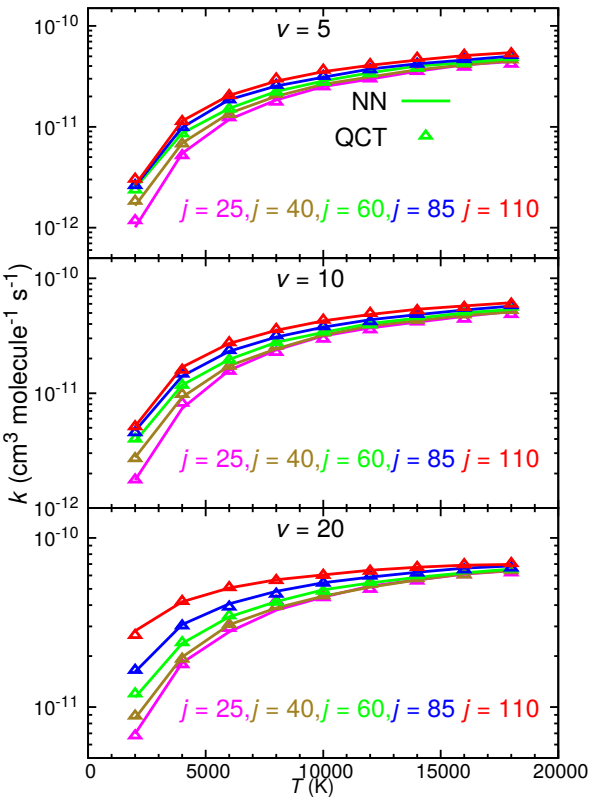

FIG. S10. Initial state specific rates calculated from QCT (reference) and predicted by NN-Tot, respectively, for the N + NO(v, j) $\rightarrow$ O + N_2 reaction at different temperatures. The symbols represent the QCT results while the solid lines represent the NN results. The top, middle and bottom panels show results for $v = 5, 10$ and 20 while the magenta, olive, green, blue and red colors represent $j = 25$, 40, 60, 85 and 110, respectively.

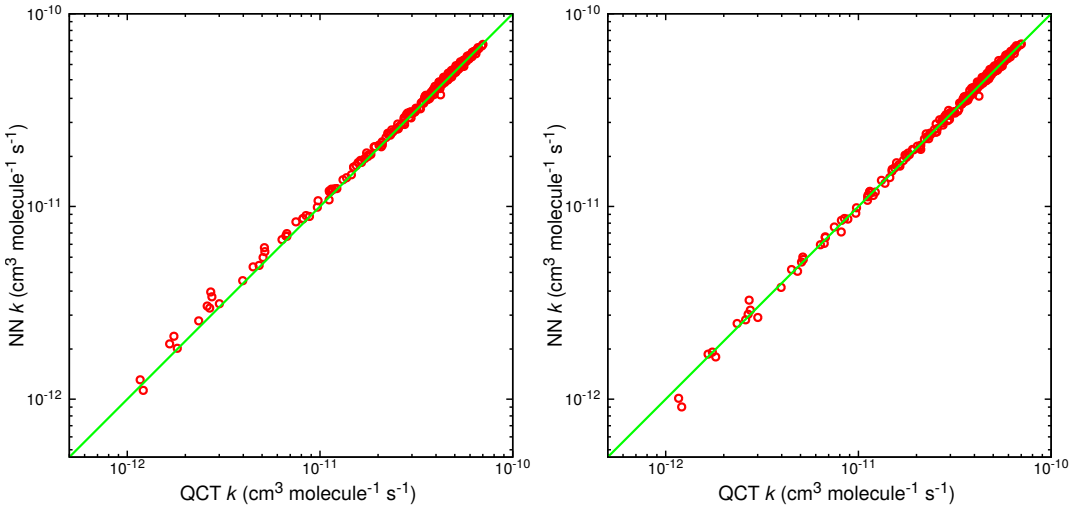

FIG. S11. Correlation between the QCT-calculated and NN-predicted initial state selected rates. Left panel: Initial state selected QCT vs NN-STS rates for $v = 5, 10, 15$ and 20, $j = 20, 25$, 40, 60, 85 and 110, and at $T =$ 2000, 4000, 6000, 8000, 10000, 12000, 14000, 16000 and 18000 K. Right panel: Total QCT vs NN-Tot rates at $T =$ 1000, 2000, 3000, 4000, 5000, 8000, 10000, 12000, 15000, 18000 and 20000 K. Diagonals are shown as solid lines.

REFERENCES

[1]O. Denis-Alpizar, R. J. Bemish, and M. Meuwly, Phys. Chem. Chem. Phys. **19**, 2392 (2017).

[2]D. G. Truhlar and J. T. Muckerman, in *Atom - Molecule Collision Theory*, edited by R. B. Bernstein (Springer US, 1979) pp. 505–566.

[3]J. D. Bender, P. Valentini, I. Nompelis, Y. Paukku, Z. Varga, D. G. Truhlar, T. Schwartzentruber, and G. V. Candler, J. Chem. Phys. **143**, 054304 (2015).